Effect of Friction Stir Processing on the Fatigue Behaviour of Cast Aluminium Alloy

Y. Uematsu[1], K. Tokaji[1], Y. Tozaki[2], H. Shibata[2], K. Fujiwara[3], T. Murayama[4]
[1]*Gifu University, Gifu, Japan;* [2]*Gifu Prefectural Research Institute for Machinery and Materials, Gifu, Japan;* [3]*Honda Motor Co., Ltd., Tokyo, Japan;* [4]*Aisin Takaoka Co., Ltd., Aichi, Japan*

1. Introduction

Cast aluminium (Al) alloys are widely used for structural components because of their advantages such as cost saving and flexibility in fabrication compared with wrought alloys. However as-cast materials generally reveal a coarse microstructure and contain many casting defects arisen from shrinkage and release of dissolved gases during solidification. Such casting defects act frequently as the crack initiation site and reduce the fatigue strength and fatigue life in cast Al alloys. From a viewpoint of fatigue reliability, therefore, controlling casting defect is extremely important, but it is very difficult to completely eliminate casting defects during casting process even though the advances in casting technology can reduce the defect size.

Friction stir processing (FSP), a variation of friction stir welding (FSW), has recently attracted special interest as an effective approach to microstructural modification after casting. By application of FSP, microstructural changes such as break-up of as-cast microstructure, grain refinement, homogenization of precipitates and elimination of casting defects are expected [1]. Thus FSP is believed to be one of the most useful methods for improving mechanical properties, particularly fatigue properties. However, there have been very limited studies on the effect of FSP on fatigue behaviour in cast Al alloys.

In the present study, FSP was applied to a cast Al alloy A356-T6 to modify the as-cast microstructure and the effect of FSP on fatigue behaviour was discussed based on microstructural consideration, crack initiation, crack growth behaviour, and fracture surface analysis.

2. Experimental procedures

2.1 Material

The material used is a cast aluminium alloy A356-T6 (AC4CH-T6 in Japanese Industrial Standard: JIS) whose chemical composition (wt.%) is Si: 6.94, Mn: 0.3, Cu: 0.016, Fe: 0.137, Ni <0.05, Ti: 0.097, Na <0.0005, Al: balance. Ageing treatment was performed at 453 K for 3 h after solution treatment at 808 K for 4 h.

2.2 FSP conditions

A tool with a 14 mm shoulder diameter and a 4.7 mm M6-threaded probe length was used in FSP. The tool was rotated clockwise and tilted 3º opposite to the processing direction. Based on preliminary tests, the tool rotational speed of 1000 rpm and the travelling speed of 150 mm/min were adopted in the present study.

FSP was performed over the whole gauge section of fatigue specimens where the processing direction coincided with the specimen axis.

2.2 Specimens

Specimen blanks of a 5 mm thickness were cut from the ingots and then friction stir processed (FSPed), from which fatigue specimens with a 8 mm width, a 12 mm gauge length and a 4 mm thickness shown in Fig.1 were machined. In order that the centre of the stir zone is positioned in the middle of the thickness, both the upper and lower surfaces were removed about 0.5 mm in depth. Fatigue specimen has a shallow notch of 45mm radius and 0.5 mm depth on the upper surface in order to facilitate the observation of crack initiation and small crack growth. Before fatigue test, the surface of the gauge section was mechanically polished using progressively finer grades of emery paper.

Three different kinds of fatigue specimens were used in fatigue tests; as-cast, FSPed (as-cast/FSP) and T6 treated after FSP (FSP/T6) where the FSPed specimen was solution treated at 808 K for 12 h and then aged at 428 K for 4 h.

2.3 Procedures

Hardness and mechanical properties were measured using a Vickers hardness tester and a material testing machine, respectively. Fully reversed axial fatigue tests were conducted on a 98 kN capacity electro-hydraulic fatigue testing machine operating at a frequency of 10 Hz in laboratory air at ambient temperature.

3. Experimental results

3.1 Microstructural modification by FSP

The microstructure of the as-cast specimen is represented in Fig.2. Typical dendrite structure with Si particles is recognized, where secondary dendrite arm spacing (SDAS) is about 19~35 μm. Small porosities shown by the arrow in Fig.2 are observed in as-cast condition

Figs.3(a) and (b) show macro and microscopic structures observed on the cross section of the as-cast/FSP specimen, respectively. The macroscopic structure consists of onion rings which are generally seen in FSW joint of Al alloys. Fig.3(b) is the magnified view at the arrow in Fig.3(a). Dendrite structure of the as-cast specimen is completely broken up by FSP and Si particles distribute uniformly. The grain refinement occurred where grain size is about 10~20 μm. Furthermore, porosities in the as-cast specimen are eliminated. Fig.4 shows the

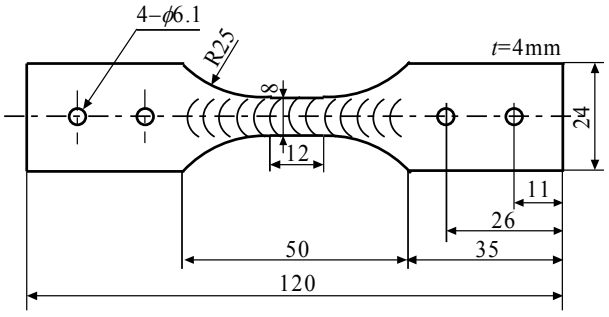

Fig.1 Fatigue specimen configuration.

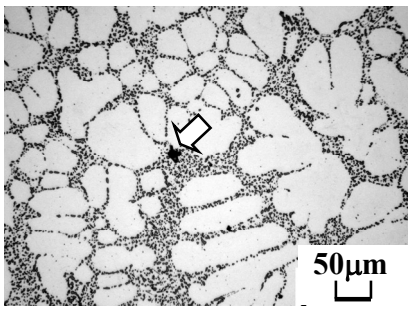

Fig.2 Microstructure of as-cast material.

macro and microscopic structures of the FSP/T6 specimen, where Fig.4(b) is the magnified view at the arrow in Fig.4(a). Onion ring pattern becomes unclear (Fig.4(a)), while distribution of Si particles is similar to that in the as-cast/FSP specimen (Fig.4(b)). It should be noted that abnormal grain growth took place in the FSP/T6 specimen. The large gain size is about 1~3mm. This kind of abnormal grain growth by post heat treatment has been also recognized in FSW joint of wrought Al alloys [2~4].

3.2 Hardness profile

The Vickers hardness profiles of the as-cast/FSP and FSP/T6 specimens are shown in Fig.5. Measurements were made along three lines of the mid-thickness,

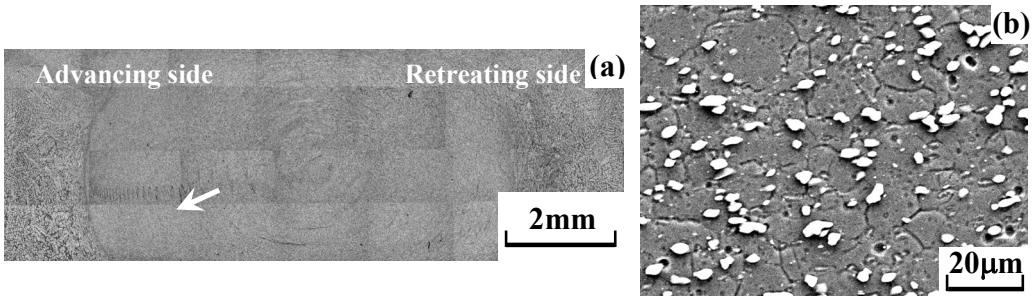

Fig.3 Microstructures of cross section in as-cast/FSP: (a) overview, (b) magnified view.

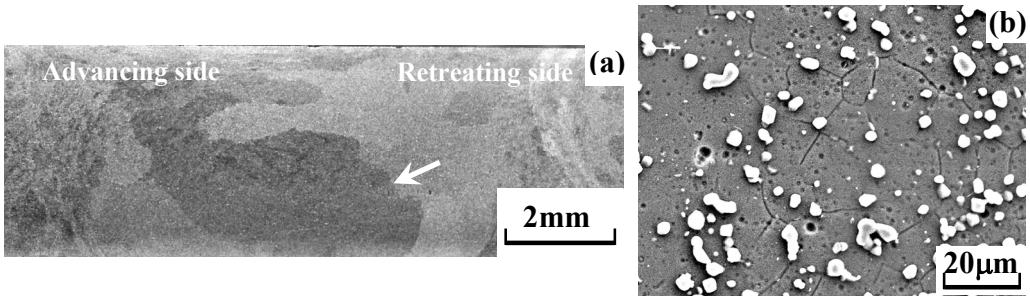

Fig.4 Microstructures of cross section in FSP/T6: (a) overview, (b) magnified view.

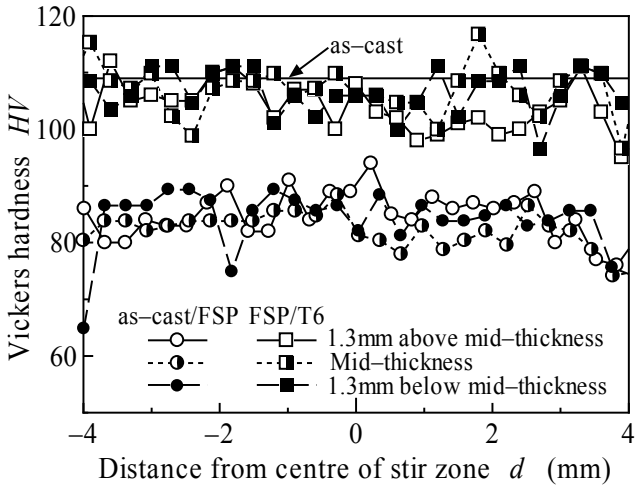

Fig.5 Vickers hardness profiles around stir zone in as-cast/FSP and FSP/T6.

1.3 mm above and below the mid-thickness on a cross section perpendicular to the specimen axis. The hardness values measured along those three lines are nearly the same. The average hardness of the as-cast specimen is shown by solid line in Fig.5 (*HV*109). The hardness of the as-cast/FSP specimen is lower than that of the as-cast one, while post T6 treatment fully recovers the hardness.

3.3 Mechanical properties

The mechanical properties of the as-cast, as-cast/FSP and FSP/T6 specimens are listed in Table 1. As generally known, the as-cast specimen has low strength and ductility. By FSP, ductility increases but proof stress and tensile strength decrease compared with the as-cast specimen. The FSP/T6 specimen exhibits higher tensile strength than the as-cast one.

3.4 Fatigue behaviour

3.4.1 Fatigue strength

The *S-N* diagram is represented in Fig.6. The as-cast specimens exhibit a large scatter, and the fatigue strength at 10^7 cycles (hereafter, fatigue limit) is 60 MPa. In the as-cast/FSP specimens, the fatigue strengths decrease in the finite life region, but the fatigue limit significantly increases to 100 MPa. The fatigue strengths of the FSP/T6 specimens in the finite life region are recovered to the similar values of the as-cast ones. On the contrary, the fatigue limit is 80 MPa and lower than the as-cast/FSP specimens, while still higher than the as-cast ones. It indicates that post heat treatment can recover the hardness, tensile strength and fatigue strength in the finite life region, but decreases fatigue limit compared with the as-cast/FSP specimen.

Table 1 Mechanical properties.

Specimen	Proof stress $\sigma_{0.2}$ (MPa)	Tensile strength σ_B (MPa)	Elongation ϕ (%)	Reduction of area ψ (%)
as-cast	164	249	12	21
as-cast/FSP	144	229	23	
FSP/T6		284	12	

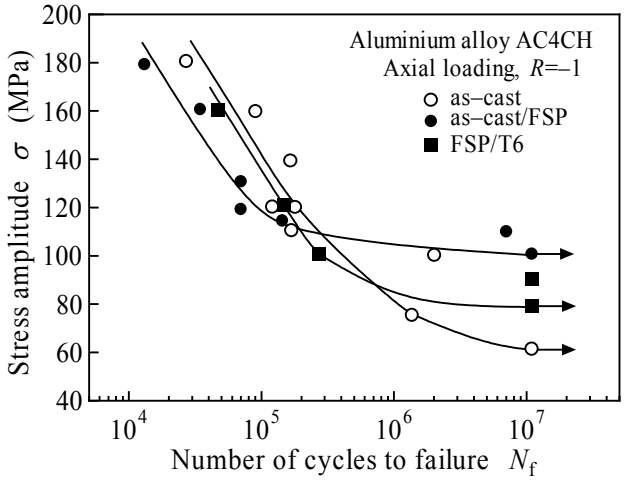

Fig.6 *S-N* diagram.

3.4.2 SEM analysis of crack initiation site

Figs. 7~9 reveal SEM micrographs of fracture surfaces near the crack initiation site in the as-cast, as-cast/FSP and FSP/T6 specimens, respectively. In the as-cast specimen (Fig.7), porosity is recognized at the crack initiation site, indicating that crack initiated from the casting defect. On the contrary, In the FSPed specimens (Figs.8 and 9), casting defects are not seen at the crack initiation sites, thus cracks were generated due to cyclic slip deformation in the matrix. It should be noted that the facet size at the crack initiation site is larger in FSP/T6 (Fig.9(b)) than in as-cast/FSP (Fig.8(b)), representing the effect of grain growth shown in Fig.4 on crack initiation.

3.4.3 Crack initiation and small crack growth

Small crack growth paths on the specimen surface are represented in Fig.10 for the as-cast, as-cast/FSP and FSP/T6 specimens, where arrows indicate the crack initiation site. In the as-cast specimen (Fig.10(a)), the crack initiated from porosity, and macroscopically grew in the direction perpendicular to the loading axis. In contrast, crack growth paths of the as-cast/FSP and FSP/T6 specimens are not straight. The etching of the specimen surface revealed the onion rings on the surface, and it is clear that crack grew along the ring in the FSPed specimens. Transverse section of the crack in FSPed specimens is observed in order to investigate the crack growth path in the depth direction, and the observation results are shown in Fig.11. In the as-cast/FSP specimen (Fig.11(a)), crack grew along the onion ring similar to the crack growth path observed on the specimen surface. In the FSP/T6 specimen, however, crack grew along the ring at the beginning but shortly penetrated those rings, which indicates that the post heat treatment decreased the sensitivity of crack growth against onion ring. Based on the observation results, crack growth path of the as-cast/FSP specimen is three-

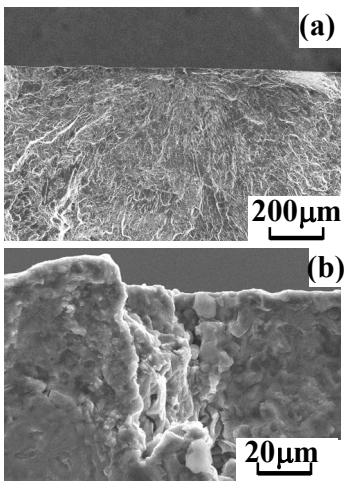

Fig.7 Fracture surface near crack initiation site in as-cast (σ=140 MPa, N_f=1.7×10^5): (a) overview, (b) magnified view.

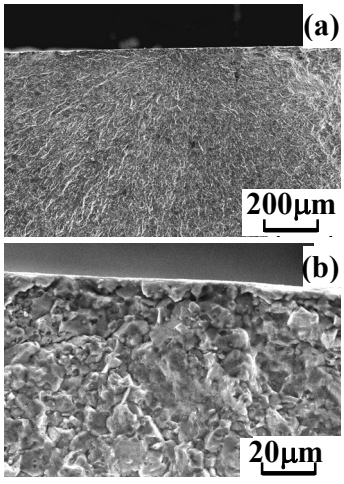

Fig.8 Fracture surface near crack initiation site in as-cast/FSP (σ= 120MPa, N_f=7.0×10^4): (a) overview, (b) magnified view.

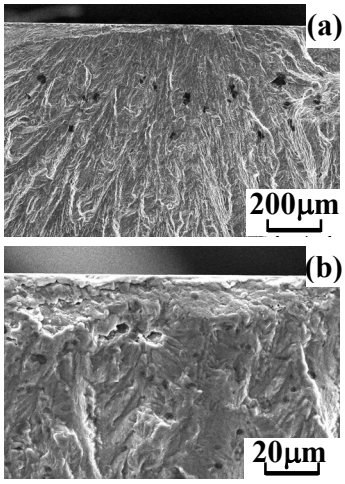

Fig.9 Fracture surface near crack initiation site in FSP/T6 (σ=100 MPa, N_f=2.7×10^5): (a) overview, (b) magnified view.

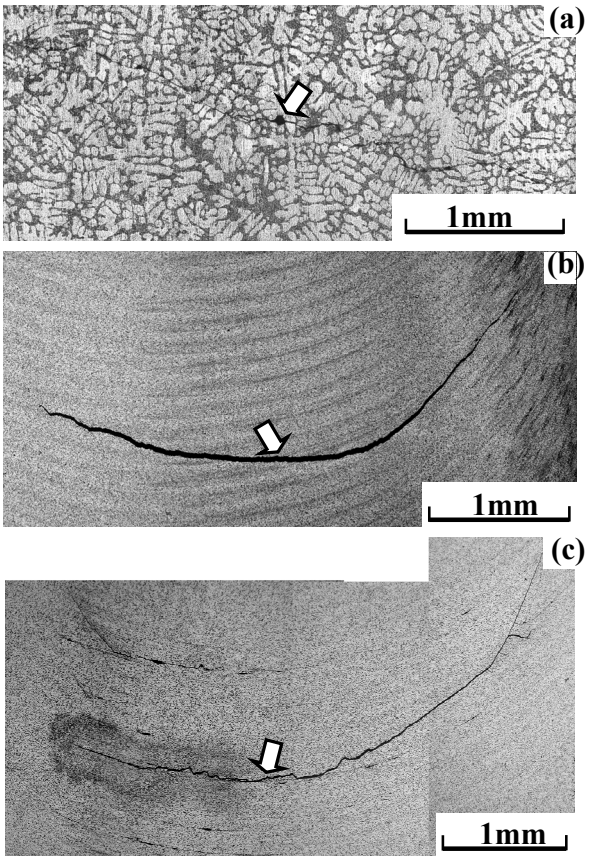

Fig.10 Macroscopic crack growth paths on specimen surface: (a) as-cast, (b) as-cast/FSP, (c) FSP/T6. The specimen axis is the vertical direction.

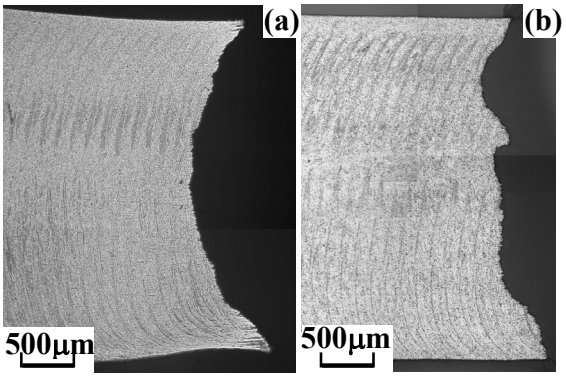

Fig.11 Macroscopic crack growth paths in thickness direction: (a) as-cast/FSP, (b) FSP/T6. The specimen axis is the horizontal direction.

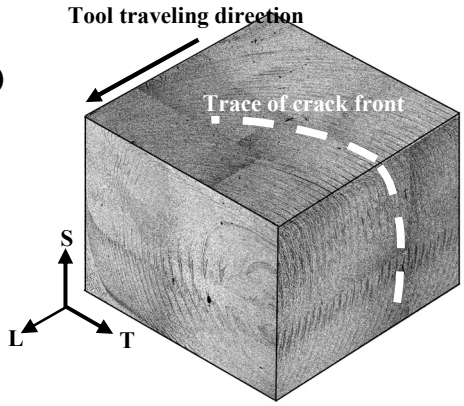

Fig.12 Three-dimensional characterization showing dependence of crack growth path on banded structure in as-cast/FSP.

dimensionally characterized in Fig.12. It indicates that FSP introduced the microstructure which could be the preferential crack growth path.

3.4.4 Crack growth behaviour

The relationship between surface crack length, 2*c*, and number of cycles, *N*, for the as-cast, as-cast/FSP and FSP/T6 specimens is illustrated in Fig.13. In the as-cast specimen, crack initiated from porosity, thus most of fatigue life is occupied by small crack growth. In the as-cast/FSP specimen, porosity was eliminated by FSP and crack initiation was due to slip deformation of matrix. Therefore, crack initiation life was highly improved. On the other hand, several cracks initiated at the beginning of the fatigue test in the FSP/T6 specimen, and crack coalescence was observed at the points shown by the arrows in Fig.13, indicating crack

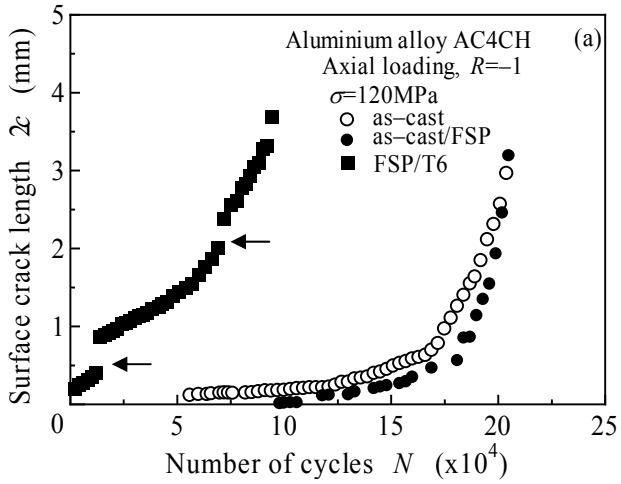

Fig.13 Crack length as a function of number of cycles.

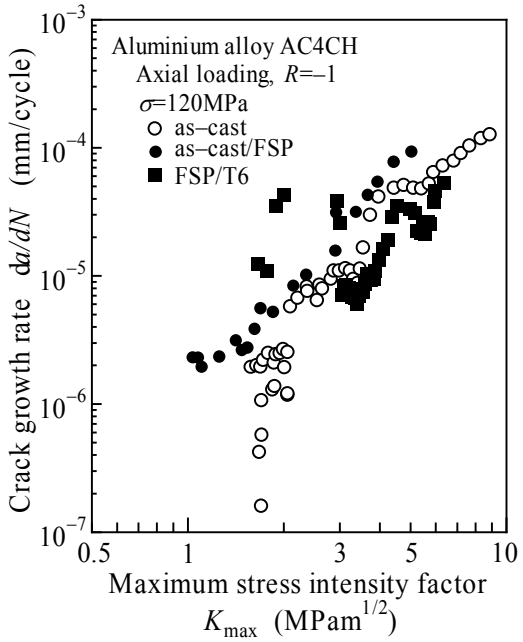

Fig.14 Relationship between crack growth rate and maximum stress intensity factor.

initiation resistance was reduced by post heat treatment. Crack growth rate, da/dN, is shown in Fig.14 as a function of maximum stress intensity factor, K_{max}, for small cracks, where crack depth, a, and K_{max} were obtained by assuming the aspect ratio of a/c=1. The crack growth rates of the as-cast/FSP specimen are slightly faster than those of the as-cast one. However, the FSP/T6 specimen exhibits slightly slower crack growth rates compared with the as-cast one excluding the effect of coalescence, and resulting in increased crack growth resistance.

4. Discussion

4.1 Effect of FSP on fatigue behaviour

As shown in Fig.6, fatigue limit was remarkably increased by FSP. It is considered that the casting defects, namely porosities, were eliminated effectively by FSP. Moreover, the dendrite structure of the as-cast specimen was broken up and the microstructure with fine grains in which Si particles distributed uniformly was developed (Fig.4). These microstructural modifications resulted in the improvement of crack initiation resistance as shown in Fig.13, and consequently the fatigue limit was enhanced by FSP. On the other hand, FSP softened the matrix due to the redissolution of precipitates by the heat input during FSP (Fig.5). Furthermore, the onion rings could be a preferential crack growth path (Fig.10(b), Fig.12(a)). Therefore, FSP decreased crack growth resistance and led to the lower fatigue strengths in the finite life region. It has been reported that onion rings were related to the texture in which {111}<110> slip systems were parallel to the rings [5], [6], and thus the fatigue crack might have grown preferentially along the onion rings. It should be noted that FSP has both favourable and unfavourable effects to fatigue properties. Elimination of porosities, uniform microstructure without dendrite and grain refinement are favourable to crack initiation resistance, while redissolution of precipitates and onion rings are unfavourable to crack growth resistance.

4.2 Effect of post heat treatment

Post heat treatment recovered fatigue strengths in the finite life region to the similar values of the as-cast specimens, while decreased fatigue limit as shown in Fig.6. But fatigue limit of the FSP/T6 specimen was still higher than that of the as-cast one. From Figs.13 and 14, it can be summarized that crack initiation resistance was reduced but crack growth resistance was enhanced by post heat treatment. From microstructural point of view, post heat treatment has brought about abnormal grain growth (Fig.4) and re-precipitation of hardening phases (Fig.5). It is considered that the abnormal grain growth reduced crack initiation resistance as represented by the larger facet size at the crack initiation site (Fig.9). On the contrary, re-precipitation increased hardness and consequently crack growth resistance. Furthermore, grain growth reduced the sensitivity of crack growth against the onion rings, in which texture was developed, as shown in Fig.11 (b), and thus had preferable effect on crack growth resistance. It is noteworthy that post heat treatment have also both favourable and unfavourable effects on fatigue properties.

5. Conclusions

Friction stir processing (FSP) was applied to cast aluminium alloy A356-T6 to modify the as-cast microstructure and then fully reversed axial fatigue tests have been performed using as-cast, FSPed and post T6 treated specimens. The effect of FSP on fatigue behaviour was discussed based on microstructural consideration, crack initiation, crack growth, and fracture surface analysis. The following conclusions can be made.

1. FSP resulted in several microstructural changes such as elimination of porosities, break-up of dendrite as-cast microstructure, grain refinement of the matrix, hardness decrease and development of onion rings.
2. Post heat treatment recovered hardness, while brought about abnormal grain growth of matrix.
3. The mechanical properties of the FSPed specimens decreased compared with the corresponding as-cast specimen, while post heat treatment achieved higher tensile strength than the as-cast one.
4. FSP enhanced fatigue limit, while decreased fatigue strengths in the finite life region compared with the as-received specimen. Post heat treatment recovered fatigue strength in the finite life region, but decreased fatigue limit.
5. Fatigue crack initiated from porosities in the as-cast specimens, while due to cyclic slip deformation of the matrix in the FSPed specimen. This transition of the crack initiation mechanism resulted in the enhanced crack initiation resistance of the FSPed specimen. Post heat treatment reduced crack initiation resistance due to the grain growth.
6. The FSPed specimen showed higher crack growth rates, while the post heat treated one exhibited lower growth rates than the as-cast one. Fatigue crack tended to grew along the onion rings introduced by FSP.

[1] Z.Y. Ma, S.R. Sharma, R.S. Mishra, Effect of Friction Stir Processing on the Microstructure of Cast A356 Aluminum, Materials Science and Engineering A433 (2006) 269-278

[2] Y.S. Sato, H. Kokawa, Distribution of Tensile Property and Microstructure in Friction Stir Weld of 6063 Aluminum, Metallurgical and Materials Transactions A 32A (2001) 3023-3031

[3] K.N. Krishnan, The Effect of Post Weld Heat Treatment on the Properties of 6061 Friction Stir Welded Joints, J Materials Science 37 (2002) 473-480

[4] Y. Uematsu, K. Tokaji, Y. Tozaki, H. Shibata, Fatigue Behaviour of Friction Stir Welded Joints of 6061-T6 Aluminium Alloy, J the Society of Materials Science, Japan 55(1) (2006) 49-54

[5] Y.S. Sato, H. Kokawa, K. Ikeda, M. Enomoto, S. Jogan, T. Hashimoto, Microtexture in the Friction-Stir Weld of an Aluminum Alloy, Metallurgical and Materials Transactions A 32A (2001) 941-948

[6] Y.S. Sato, H. Kokawa, Materials Science in Friction Stir Welding, Materia Japan 42 (2003) 214-220.